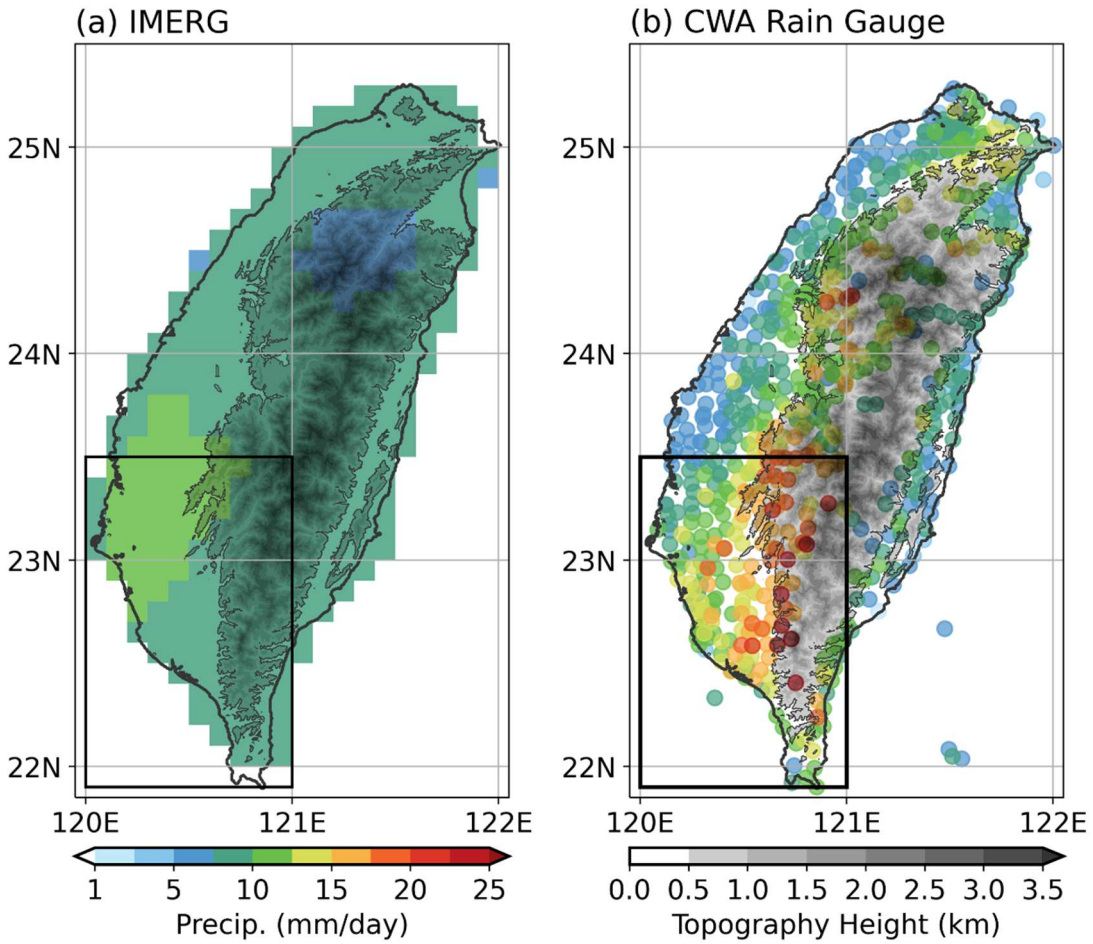

Figure S1: Rainfall pattern comparison between IMERG and CWA rain gauges. The rainfall value is averaged over April–September 2001–2019. The high-resolution (500 m) coastline and topography are retrieved from the settings of TaiwanVVM. Rainfall values near the foothills and beyond are apparently underestimated, especially over the southwestern area (solid-line box).

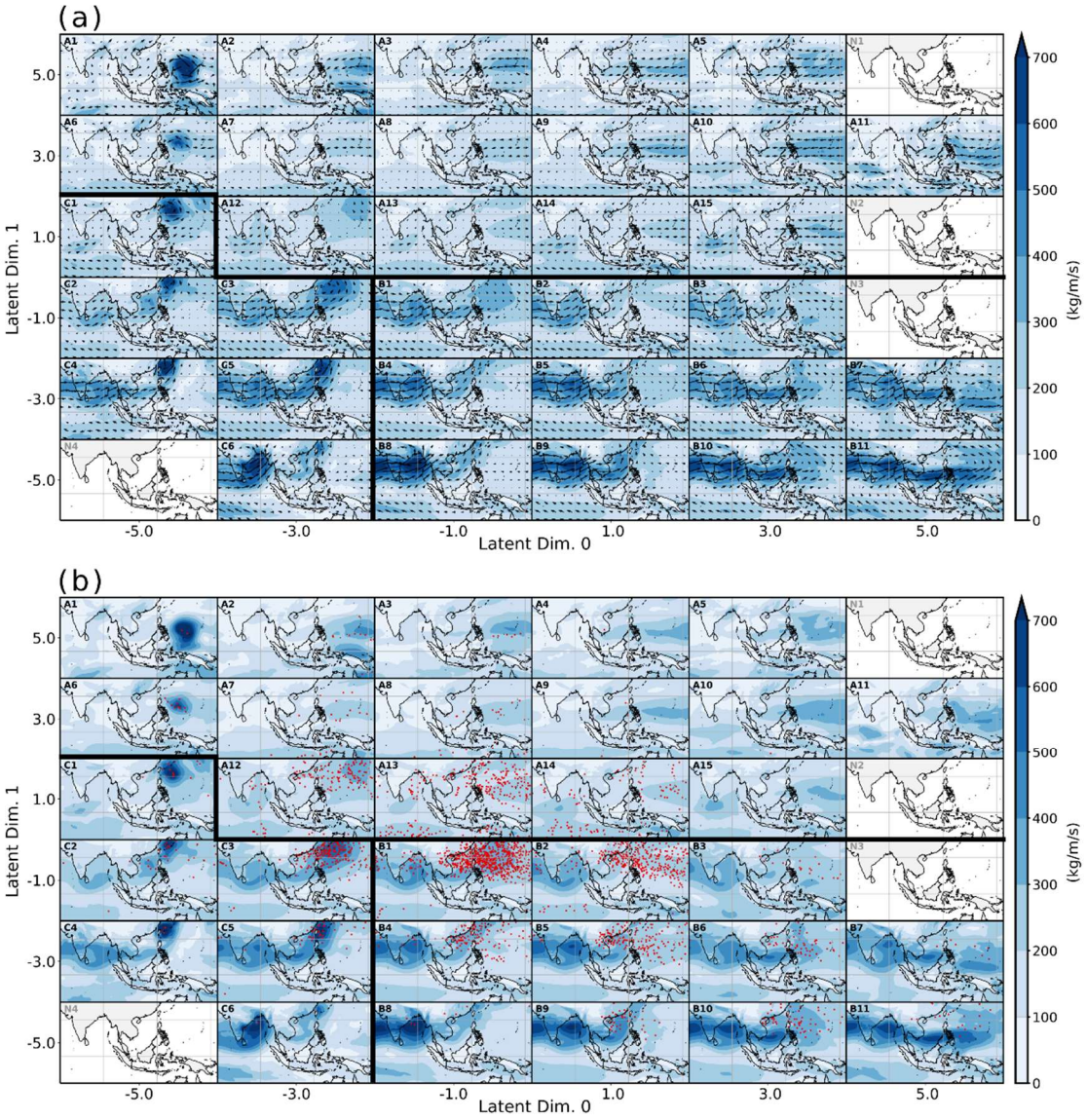

Figure S2: Sample composites of the 36 large-scale IVT regimes. Shading illustrates the composite IVT intensity, identical in both panels. Arrows in (a) denote the IVT vectors. Red dots in (b) denote the documented tropical cyclone positions from IBTrACS (see Section 2.1). The five empty subspaces (with N-initials) in Fig. 3b correspond to the five blank subplots here.

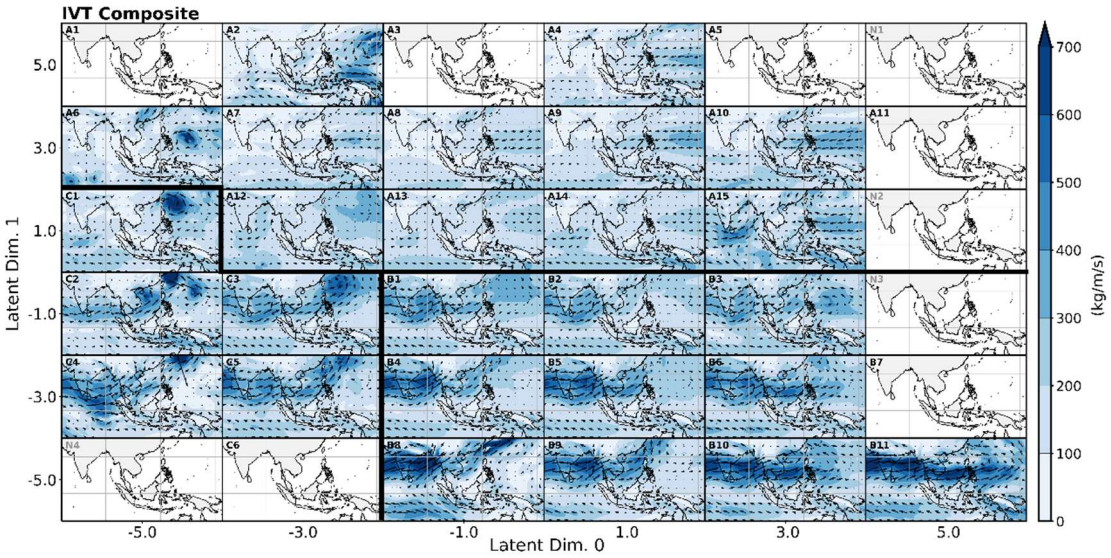

Figure S3: Similar to Fig. S2a but only with testing samples.

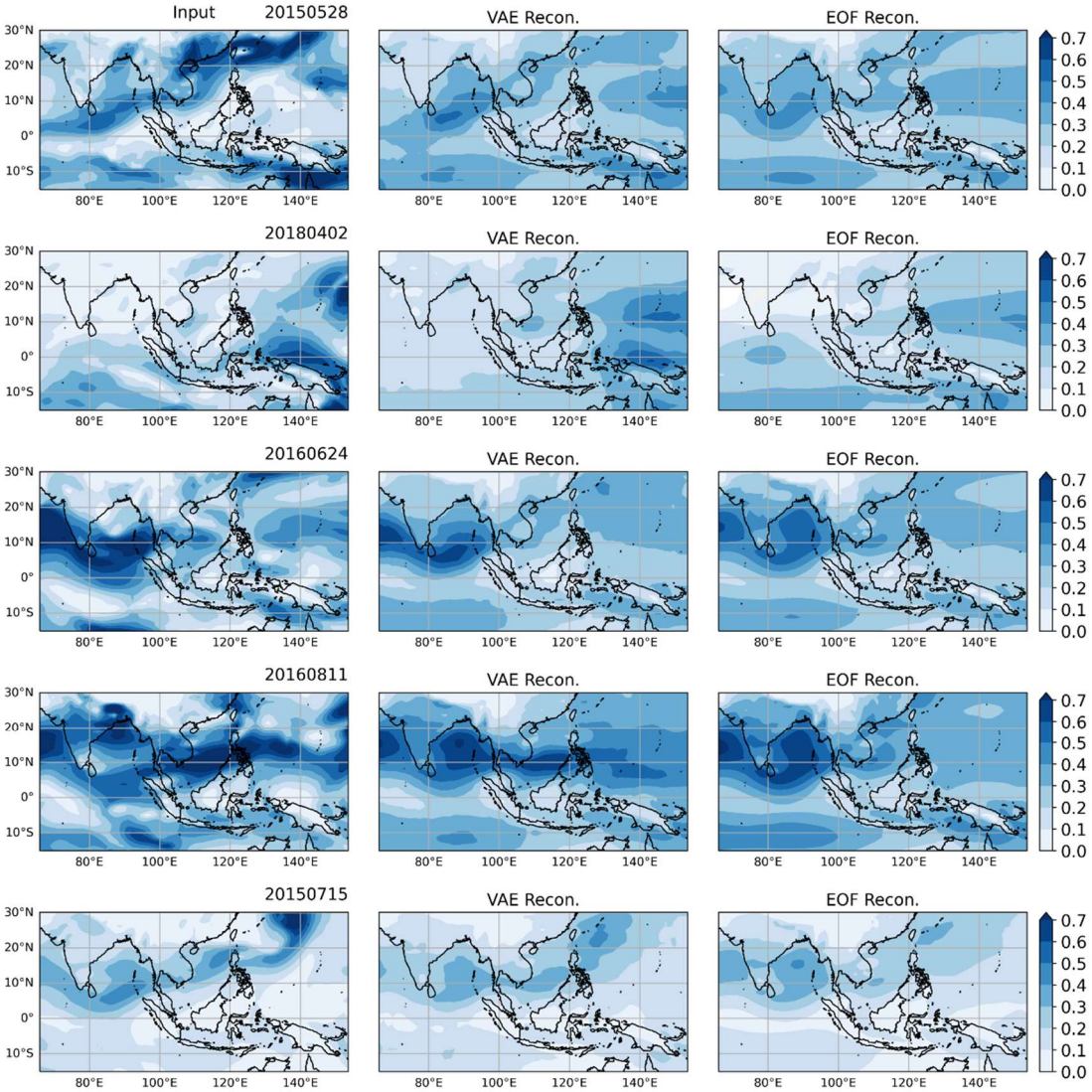

Figure S4: Five distinct daily IVT patterns demonstrating VAE reconstructions versus EOF. Normalized input fields are on the leftmost column, VAE reconstructions in the middle, and the EOF reconstructions on the rightmost column. The inputs of VAE and EOF are identical, and both of them are constrained to reconstruct samples with two dimensions. VAE is capable of capturing and representing more details of different spatial scales than EOF, and thus the reconstructions from VAE bear higher resemblance to the input fields.

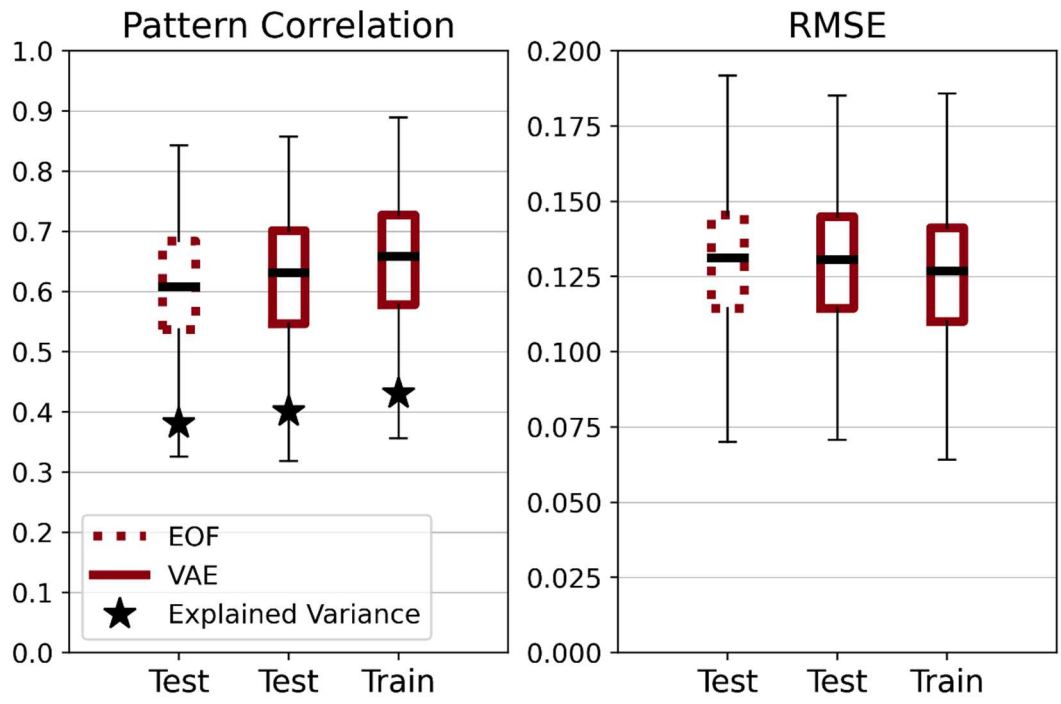

Figure S5: Pattern correlation and root mean square error distribution between the ERA5 input samples and reconstruction. Labels on the x-axis denote the samples subset. VAE performs on the unseen testing subset well and better than EOF, providing credibility for our further analyses.

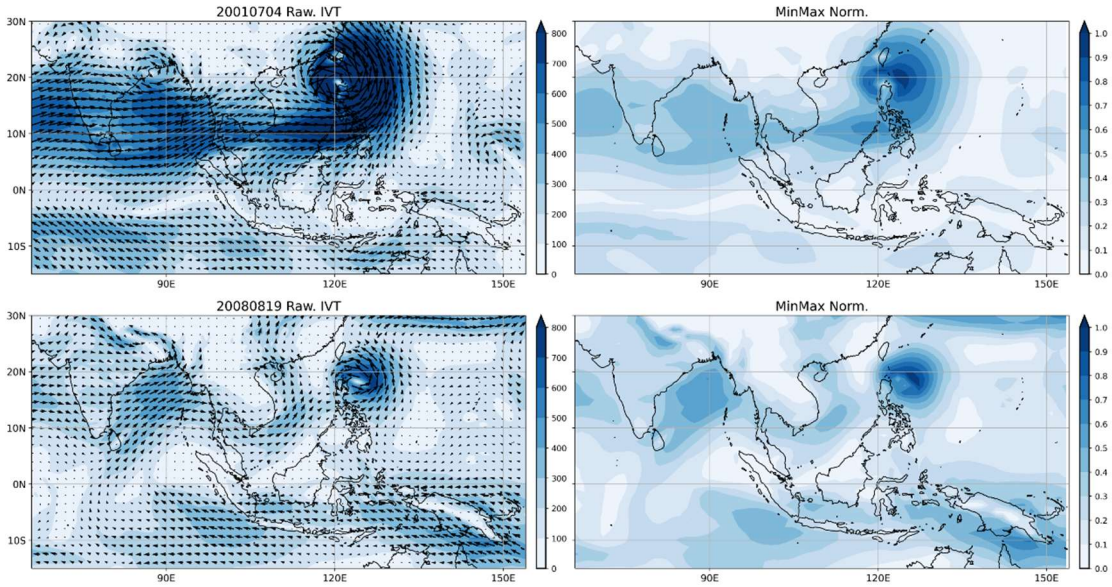

Figure S6: Example of two daily IVT patterns sharing similar patterns but distinct overall intensities. Both samples are classified into the B1 regime by VAE (Fig. 3c). Left panels show the original fields, whereas the right ones are the individually normalized patterns and are also the inputs of VAE.

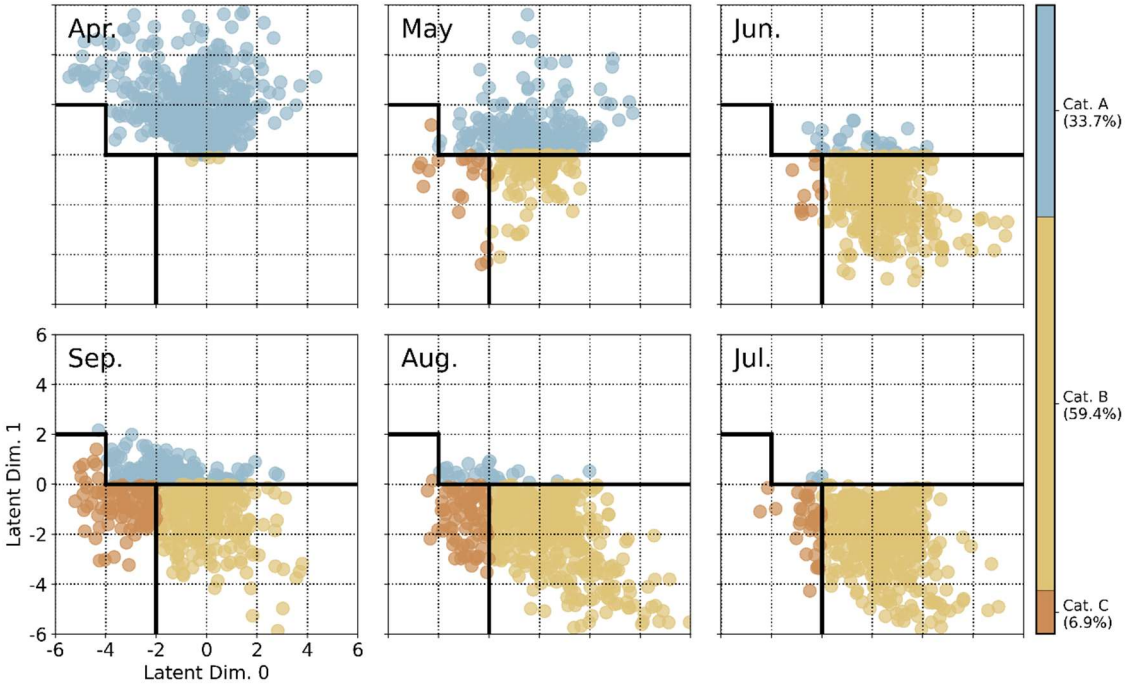

Figure S7: Distribution of daily IVT patterns over the identified large-scale IVT regimes in each summer month. Colors denote the three categories. Panels are arranged clockwise chronologically starting from the upper left.

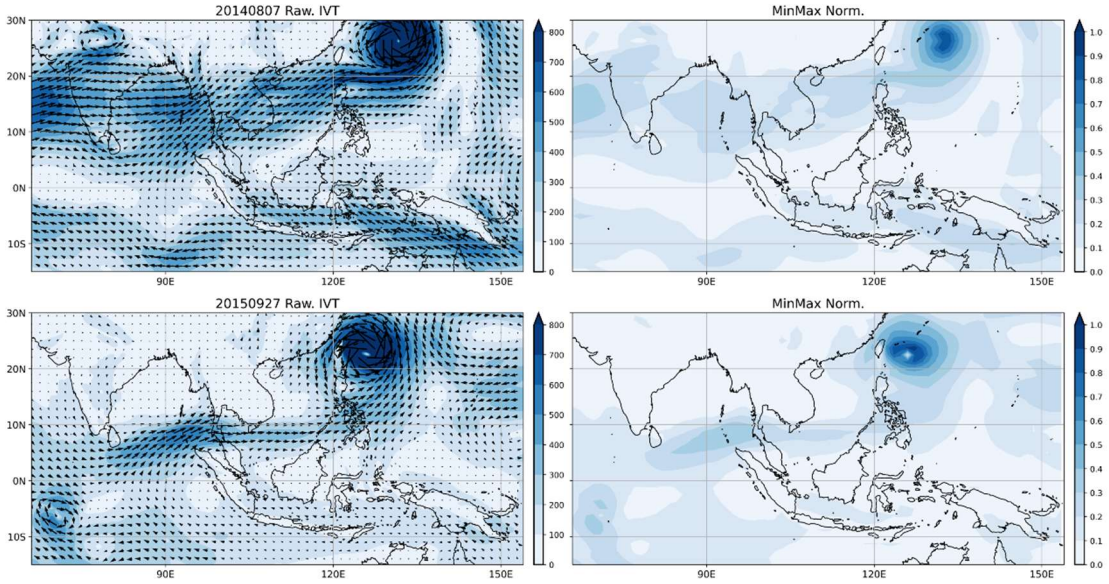

Figure S8: Two examples from the C3 large-scale IVT regime. Left panels show the original fields, whereas the right ones are the individually normalized patterns and are also the inputs of VAE. Due to the concentrated IVT cores of tropical cyclones, the overall normalized intensity pattern can appear relatively weak.

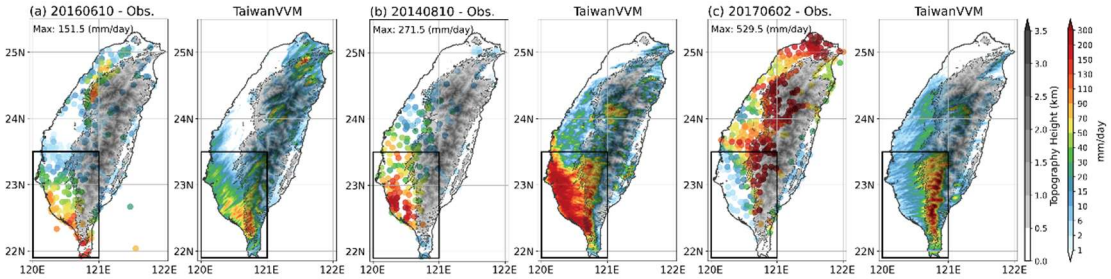

Figure S9: Another set of upstream-inflow dominant cases with varying spatial patterns, well-reproduced by TaiwanVVM. Left (right) panel of each subplot shows the observed (TaiwanVVM-simulated) pattern.

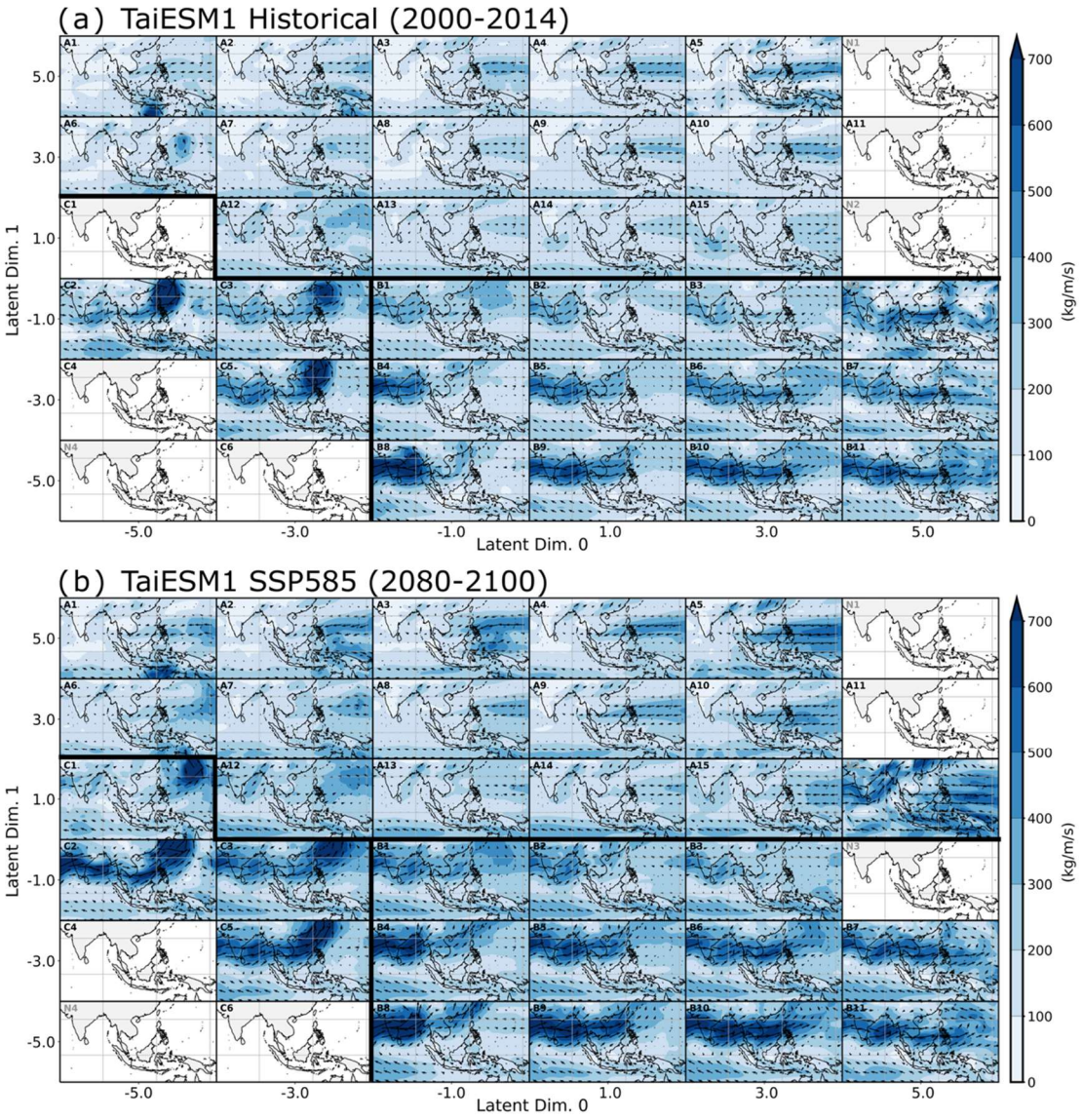

Figure S10: Similar to Fig. S2a but with TaiESM1-simulated IVT. (a) is derived from historical data (2001–2014) and (b) from the SSP5-8.5 future scenario (2080–2100).

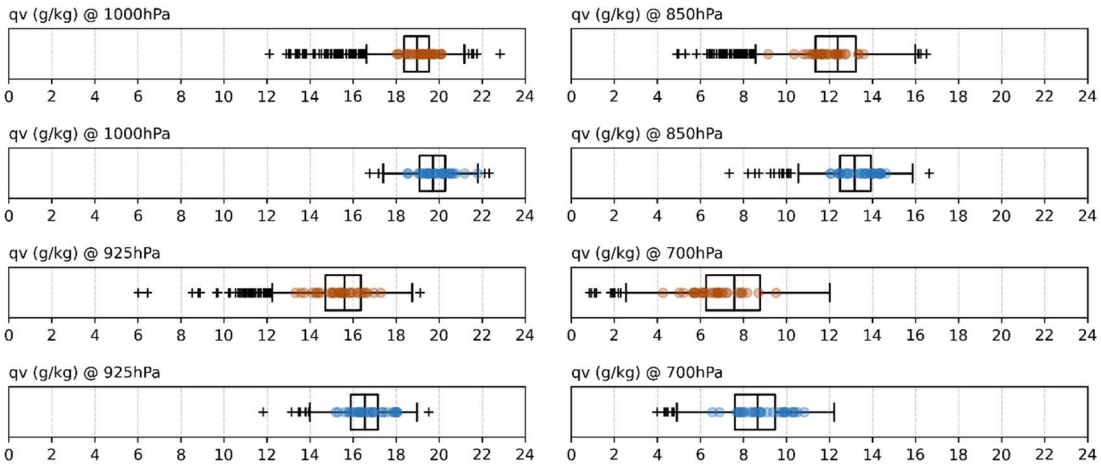

Figure S11: Specific humidity ranges throughout the low levels (1000–700 hPa). Similar to the bottom panels in Fig. 6a and 6d, where plots with orange (blue) dots represent local-circulation (upstream-inflow) dominant cases.